Observation of the Rare Baryonic Decay $B^+ \to p\bar{\Lambda}$ and Measurement of its Weak Decay Parameter

R. Aaij *et al.*[*]
(LHCb Collaboration)

(Received 2 December 2025; revised 7 January 2026; accepted 9 January 2026; published 6 February 2026)

The first observation of the decay $B^+ \to p\bar{\Lambda}$ is presented using proton-proton collision data collected by the LHCb experiment between 2016 and 2018 at a center-of-mass energy of 13 TeV, corresponding to an integrated luminosity of 5.4 fb^{-1}. The signal significance exceeds seven standard deviations. Using the $B^+ \to K^0_S\pi^+$ decay as a normalization channel, the branching fraction is measured and combined with previous LHCb results based on data collected at 7 and 8 TeV in 2011 and 2012, yielding $\mathcal{B}(B^+ \to p\bar{\Lambda}) = (1.24 \pm 0.17 \pm 0.05 \pm 0.03) \times 10^{-7}$, where the first uncertainty is statistical, the second is systematic, and the third comes from the uncertainty on the branching fraction of the normalization channel. The $B^+ \to p\bar{\Lambda}$ weak decay parameter is measured to be $\alpha_B = 0.87^{+0.26}_{-0.29} \pm 0.09$, indicating the presence of comparable S-wave and P-wave decay amplitudes.

DOI: 10.1103/fj4q-t8jg

The study of charmless two-body B-meson decays provides critical insights into strong interaction dynamics and CP violation in heavy-quark decay processes. While decays into a pseudoscalar-meson pair ($B \to PP'$) have been extensively examined by the *BABAR* [1–4], Belle [5–8], and LHCb [9–14] collaborations, decays into a baryon-antibaryon pair are significantly less explored. Prior to this Letter, only two such processes had been observed, $B^0 \to p\bar{p}$ [15] and $B^+ \to p\bar{\Lambda}(1520)$ [16], and precise measurements of their decay properties are lacking.

Following pioneering searches conducted by the CLEO [17] and Belle [18] collaborations, the LHCb experiment reported the first evidence for the $B^+ \to p\bar{\Lambda}$ decay with a significance of 4.1σ using proton-proton (pp) collision data collected at center-of-mass energies of 7 and 8 TeV during 2011–2012 (Run 1) [19]. (The symbol Λ is used to refer to the ground-state Λ baryon, and the inclusion of charge-conjugate processes is implied, throughout this Letter.) The measured branching fraction, $\mathcal{B}(B^+ \to p\bar{\Lambda}) = (2.4^{+1.0}_{-0.8} \pm 0.3) \times 10^{-7}$, was found to be in good agreement with the theoretical predictions [20,21], although improved experimental precision is highly desirable. This would help to better constrain the tree-level and loop (penguin) amplitudes in charmless two-body baryonic B-meson decays [22], which allows for more reliable predictions of their decay rates and CP asymmetries. Improved precision is also useful for testing various near-threshold enhancement mechanisms [23–25] proposed to explain why two-body B-meson decays to baryons are significantly suppressed relative to their multibody counterparts.

Furthermore, clearly observing the $B^+ \to p\bar{\Lambda}$ decay will be a key step toward studies of CP violation in this decay, which may potentially help resolve an intriguing anomaly regarding the magnitude of CP violation observed in the $\Lambda_b^0 \to pK^-$ decay. These two decays, as well as the $B_s^0 \to K^+K^-$ and $B^0 \to K^+\pi^-$ decays, are related by the underlying $\bar{b} \to u\bar{u}\,\bar{s}$ quark transition. The representative diagrams for $B^+ \to p\bar{\Lambda}$ are illustrated in Fig. 1. Sizable CP-violation effects can arise from the interference between tree-level and penguin contributions of similar size [26]. While the $B_s^0 \to K^+K^-$ and $B^0 \to K^+\pi^-$ decays exhibit CP asymmetries of $\sim$10% [13], the recent measurement of $A_{CP}(\Lambda_b^0 \to pK^-) = (-1.14 \pm 0.76)\%$ [27] by the LHCb collaboration reveals a puzzling suppression. This anomaly may stem from cancellation of CP asymmetries between different partial waves [26,28]—a unique feature present in b-hadron decays involving baryons but absent in $B \to PP'$ processes. Theoretical studies have suggested that the CP asymmetry in $B^+ \to p\bar{\Lambda}$ could reach the 10% level [22], but this could be suppressed by cancellation between the S-wave and P-wave amplitudes [29], A_S and A_P, corresponding to the decays to states with orbital angular momentum $L = 0$ and $L = 1$ between the proton and the $\bar{\Lambda}$ baryon. However, this cancellation necessitates both sizable S-wave and P-wave amplitudes. An angular analysis measuring the weak decay parameter $\alpha_B = 2\mathcal{R}e(A_S \cdot A_P)/(|A_S|^2 + |A_P|^2)$ [26], which

[*]Full author list given at the end of the Letter.

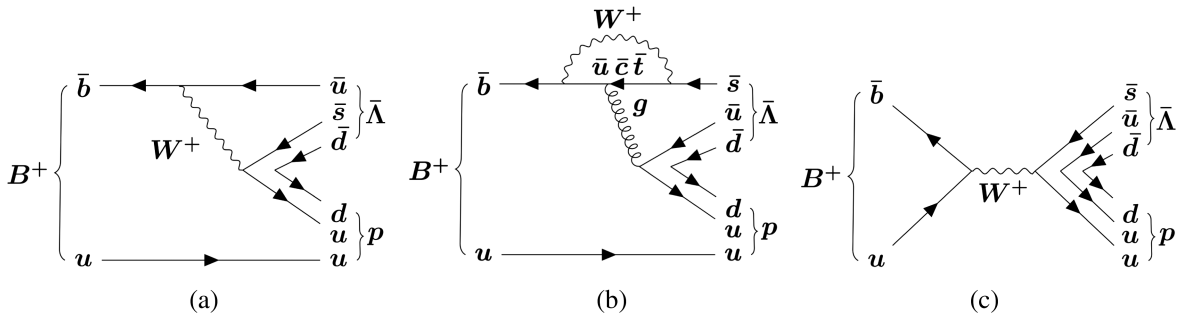

FIG. 1. Representative Feynman diagrams for the $B^+ \to p\bar{\Lambda}$ decay. (a) Tree-level. (b) Penguin. (c) Annihilation.

characterizes the interference between the two amplitudes, can test this assumption. Therefore, experimental investigation of the CP violation and angular distribution in $B^+ \to p\bar{\Lambda}$ decays can provide valuable insights to elucidate the situation.

This Letter presents the first observation of the rare baryonic decay $B^+ \to p\bar{\Lambda}$ and the first measurement of its decay parameter using pp collision data collected during 2016–2018 (Run 2) by the LHCb experiment at a center-of-mass energy of 13 TeV, corresponding to an integrated luminosity of 5.4 fb^{-1}. The branching fraction of the $B^+ \to p\bar{\Lambda}$ decay was measured relative to the normalization decay $B^+ \to K^0_S\pi^+$, with subsequent decays $\bar{\Lambda} \to \bar{p}\pi^+$ and $K^0_S \to \pi^+\pi^-$. This result was then combined with the previous LHCb measurement. In order to avoid experimenter's bias, the results of the analysis were not examined until the full analysis procedure had been finalized.

The LHCb detector is a single-arm forward spectrometer covering the pseudorapidity range $2 < \eta < 5$, described in detail in Refs. [30,31]. Of particular relevance for this analysis is the tracking system. Depending on the decay vertex position of the V^0 (representing $\bar{\Lambda}$ or K^0_S) particle, the decay products can be reconstructed as *long* tracks using hits from the full tracking system or as *downstream* tracks without hits in the vertex detector. This analysis uses V^0 decays reconstructed from either two long tracks (LL) or two downstream tracks (DD). Due to their difference in the invariant-mass resolution, B^+ candidates formed with these two types of V^0 hadrons are analyzed separately. Particle identification (PID) information is provided by two ring-imaging Cherenkov detectors.

Simulation is used to develop the selection strategy, model the signal and background invariant-mass distributions, and evaluate the efficiencies for the measurement of the relative branching fraction. Signal and normalization decays are generated uniformly in phase space using the software described in Refs. [32–36]. The simulated kinematic spectra of the B^+ mesons, angular distribution of the final-state particles, as well as the track multiplicity, are corrected to match those observed in the data. The PID response in the simulation is also tuned to match that in the data using dedicated calibration samples [37].

The online event selection [38] is performed by a trigger [39], which consists of a hardware stage, based on information from the calorimeter and muon systems, followed by two software stages, which apply a partial and full event reconstruction. The hardware trigger decisions are classified as trigger on signal (TOS) if only signal tracks are used in the trigger decision or as trigger independent of signal (TIS) if particles independent of the signal, such as high energy leptons or photons from the decay of the other b-hadron, are used to select the event. Subsequently, the software trigger requires a two- or three-track secondary vertex with a significant displacement from any primary pp interaction vertex (PV).

In the offline selection, four independent subsamples of B^+ candidates are formed for each decay mode, corresponding to the combinations of two trigger categories (TOS and TIS) and two track categories (LL and DD). Due to their different background levels and compositions, these categories are analyzed separately in the selection and mass fit procedures, but they are combined for the angular analysis.

The V^0 candidates, reconstructed using pairs of oppositely charged tracks under the $\bar{p}\pi^+$ or $\pi^+\pi^-$ particle hypothesis, must have a good-quality decay vertex that is significantly displaced from any PV and meet minimum momentum thresholds. The reconstructed invariant mass is required to fall in the window $[1112, 1120]$ MeV/c^2 ($[1110, 1122]$ MeV/c^2) for the LL (DD) category under the $\bar{p}\pi^+$ hypothesis for $\bar{\Lambda}$ candidates and $[480, 515]$ MeV/c^2 ($[465, 530]$ MeV/c^2) under the $\pi^+\pi^-$ hypothesis for K^0_S candidates. Subsequently, the V^0 candidates are further combined with a proton (pion) for the signal (normalization) channel to reconstruct B^+ candidates. The B^+ and V^0 decay vertices are required to be separated by at least 2.5 standard deviations along the beam direction. Since the momentum vector of a B^+ candidate should point back to the production vertex, the candidate is required to have a small opening angle between its momentum and flight direction and a small χ^2_{IP} with respect to the associated PV. Here, the associated PV is the PV that is best aligned with the B^+ flight direction, and χ^2_{IP} is the difference between the vertex-fit χ^2 of the given PV reconstructed with and without the particle in question. A

kinematic fit is performed to improve the B^+ mass resolution by constraining the invariant mass of the V^0 candidate to the known $\bar{\Lambda}$ (K^0_S) mass [40] and requiring the B^+ candidate to originate from the associated PV.

Due to possible misidentification of a charged pion as a proton, or vice versa, $K^0_S \to \pi^+\pi^-$ and $\psi(2S) \to p\bar{p}$ (only in the LL case) decays can be mistakenly reconstructed as $\bar{\Lambda} \to \bar{p}\pi^+$ decays. These background candidates are suppressed using PID information or rejected by dedicated vetoes in the corresponding mass spectra. Similarly, for the $B^+ \to K^0_S\pi^+$ mode, backgrounds from $K^*(892)^0 \to K^+\pi^-$ (LL only), $\bar{\Lambda} \to \bar{p}\pi^+$, and $D^0 \to K^-\pi^+$ (LL only) arise when a charged kaon or proton is misidentified as a pion, and these candidates are vetoed.

For each B^+ decay mode and data category, a multivariate classifier based on the boosted decision tree (BDT) [41,42] method is employed to differentiate the signal from combinatorial background composed of random combinations of tracks. The classifier is trained using simulated signal decays and background from the high-invariant-mass sideband ($[5700, 6000]\ \mathrm{MeV}/c^2$) of selected B^+ data candidates. The BDT classifier mainly uses information on the decay kinematics and topology of the B^+ decay chain as well as PID information for the charged hadron originating directly from the B^+ decay. The optimal requirement on the BDT response of the $B^+ \to p\bar{\Lambda}$ candidates is determined by maximizing the figure-of-merit $\epsilon/[(\mathrm{X}/2) + \sqrt{N_B}]$ [43], where ϵ is the signal efficiency of the BDT requirement obtained from simulation, X is the target significance (set to 5), and N_B is the background yield in the invariant-mass signal region defined to be within three times the resolution from the known B^+ mass [40]. The BDT requirement for the $B^+ \to K^0_S\pi^+$ mode is optimized by maximizing the quantity $N_S/\sqrt{N_S + N_B}$, where N_S denotes the expected signal yield. After applying all the selection criteria discussed above, all candidates in the B^+ invariant-mass region $[5040, 5700]\ \mathrm{MeV}/c^2$ are retained for the subsequent analysis.

To determine the signal yields, a simultaneous unbinned maximum-likelihood fit is performed for each data category on both the $p\bar{\Lambda}$ and $K^0_S\pi^+$ mass distributions. The $p\bar{\Lambda}$ mass spectrum consists of a signal peak, a combinatorial background component, and partially reconstructed structures appearing in the low-mass region. The $K^0_S\pi^+$ mass spectrum features an additional misidentification background from $B^+ \to K^0_S K^+$ decays.

For both decay modes, the signal peak is described by the sum of a double-sided crystal-ball (DSCB) function [44] and a Gaussian function. The tail parameters, the relative fractions of the two functions, and the ratio of their widths are fixed to values obtained from simulation. The combinatorial background is described by an exponential function, with the slope parameter determined from the fit to each mass spectrum. Partially reconstructed backgrounds populating the $B^+ \to p\bar{\Lambda}$ lower-mass sideband are assumed to arise from $B^0 \to p\bar{\Lambda}\pi^-$, $B^+ \to p\bar{\Lambda}\pi^0$, and $B^+ \to p\bar{\Lambda}\gamma$ decays. Their shapes are derived from simulation and modeled using a kernel density estimation [45]. In the $K^0_S\pi^+$ mass spectrum, the partially reconstructed background is modeled empirically by an ARGUS function [46] convolved with a Gaussian function. Furthermore, the background due to misidentified $B^+ \to K^0_S K^+$ decay is modeled by a DSCB function, with the tail parameters and the mass difference between the $B^+ \to K^0_S K^+$ and $B^+ \to K^0_S\pi^+$ peaks fixed to values obtained from simulation.

In the simultaneous fit, the $B^+ \to p\bar{\Lambda}$ and $B^+ \to K^0_S\pi^+$ signal models share a common peak position and a scale factor that describes potential differences in mass resolution between data and simulation. The yields of all components are allowed to vary in the fit except the yield of the misidentification background from $B^+ \to K^0_S K^+$ decays, which is fixed based on the $B^+ \to K^0_S K^+$ to $B^+ \to K^0_S\pi^+$ branching fraction ratio and the relative efficiencies determined from simulation.

The obtained yields of $B^+ \to p\bar{\Lambda}$ and $B^+ \to K^0_S\pi^+$ decays in each data category are given in the End Matter. The total signal yield is determined to be 88 ± 12 for the $B^+ \to p\bar{\Lambda}$ decay and $(28.5 \pm 0.2) \times 10^3$ for the $B^+ \to K^0_S\pi^+$ process, where the uncertainties are statistical only. The invariant-mass distributions for both B^+ decay modes, summing over all four data categories, are shown in Fig. 2 along with the fit results. The statistical significance of the $B^+ \to p\bar{\Lambda}$ decay, evaluated using the likelihood-ratio test [47] and combining the four subsamples, exceeds seven standard deviations. The log-likelihood curve is shown in the End Matter. The fit results are used to subtract the background in the subsequent angular analysis using the *sPlot* technique [48]. The outcome of the angular analysis is, in turn, used to determine the decay branching fraction, as described later.

The weak decay parameter α_B can be obtained from an analysis of the angular distribution described by [49],

$$\frac{\mathrm{d}N}{\mathrm{d}\cos\theta_p} \propto (1 - \alpha_\Lambda \alpha_B \cos\theta_p) \cdot \epsilon(\cos\theta_p),$$

where θ_p denotes the angle between the antiproton momentum and the direction opposite to the B^+ momentum in the $\bar{\Lambda}$ rest frame, and α_Λ is the weak decay parameter of the $\Lambda \to p\pi^-$ process, for which the CP-average value $\alpha^{\mathrm{avg}}_\Lambda = 0.754 \pm 0.003$ reported by the BESIII experiment is used [50]. The acceptance function $\epsilon(\cos\theta_p)$ accounts for the effect of the detector geometry and selection requirements. Its shape is obtained from simulation and described using a second-order polynomial function. The background-subtracted angular distribution and the acceptance shape are presented in Fig. 3. An unbinned maximum-likelihood fit to the background-subtracted data [51] is

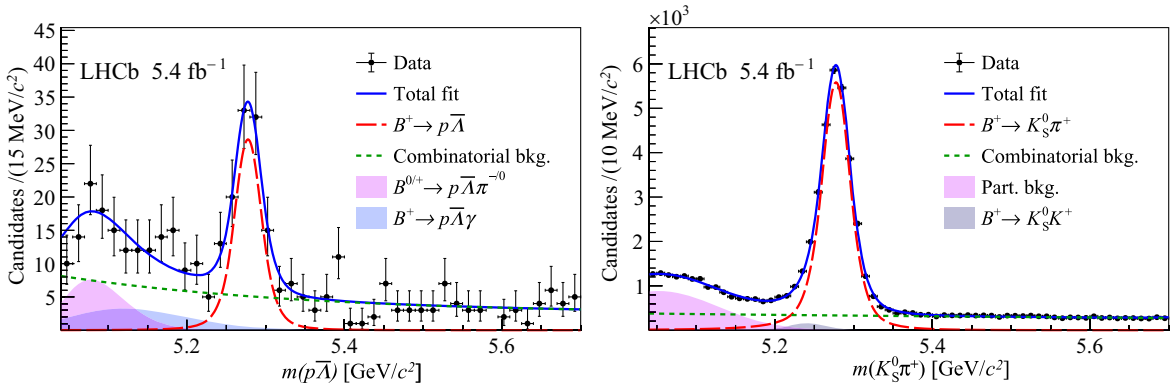

FIG. 2. Invariant-mass distributions of selected (left) $B^+ \to p\bar{\Lambda}$ and (right) $B^+ \to K^0_S\pi^+$ candidates combining all categories. The results of the fit are also shown.

performed to extract the decay parameter α_B. The angular fit procedure is validated using pseudoexperiments, and a small bias in the estimate of α_B is observed and assigned as a systematic uncertainty. The evaluation of the acceptance shape from simulation is verified using the $B^+ \to K^0_S\pi^+$ control channel, for which the distribution of the cosine of the π^+ helicity angle in the K^0_S rest frame is known to be flat. Systematic uncertainties associated with the modeling of the acceptance shape and the signal and background mass shapes are assessed by using alternative models, while biases due to the assumption of no correlation between the $p\bar{\Lambda}$ mass and the angular variable $\cos\theta_p$ are evaluated by performing separate mass fits in different ranges of $\cos\theta_p$ and recalculating the signal weights. The resulting shifts of the α_B value are assigned as the corresponding systematic uncertainties and summed in quadrature. The uncertainty originating from the Λ weak decay parameter is found to be negligible. The decay parameter is measured to be

$$\alpha_B = 0.87^{+0.26}_{-0.29} \pm 0.09,$$

where the first uncertainty is statistical and the second is systematic. This result is consistent with the theoretical prediction of $\alpha_B \approx 0.6$ [29].

The branching fraction of the $B^+ \to p\bar{\Lambda}$ decay is measured with respect to that of the $B^+ \to K^0_S\pi^+$ decay following the equation

$$\mathcal{R} \equiv \frac{\mathcal{B}(B^+ \to p\bar{\Lambda})}{\mathcal{B}(B^+ \to K^0_S\pi^+)} = \frac{N(B^+ \to p\bar{\Lambda})}{N(B^+ \to K^0_S\pi^+)} \cdot \frac{\epsilon(B^+ \to K^0_S\pi^+)}{\epsilon(B^+ \to p\bar{\Lambda})} \cdot \frac{\mathcal{B}(K^0_S \to \pi^+\pi^-)}{\mathcal{B}(\bar{\Lambda} \to \bar{p}\pi^+)}.$$

Here, $\mathcal{B}(K^0_S \to \pi^+\pi^-) = (69.20 \pm 0.05) \times 10^{-2}$ and $\mathcal{B}(\Lambda \to p\pi^-) = (64.10 \pm 0.50) \times 10^{-2}$ are taken from Ref. [40], N denotes the yield of the signal or normalization channel extracted from the data fits, and ϵ represents the total reconstruction and selection efficiency, which is determined for each decay mode using corrected simulation samples.

Systematic uncertainties on the branching fraction ratio associated with the fitting procedure and the efficiency determination are summarized in Table I. Pseudoexperiments are performed to validate the mass fit procedure. A bias in the $B^+ \to p\bar{\Lambda}$ yield is found and assigned as a systematic uncertainty. The systematic uncertainty resulting from the choice of fit model is

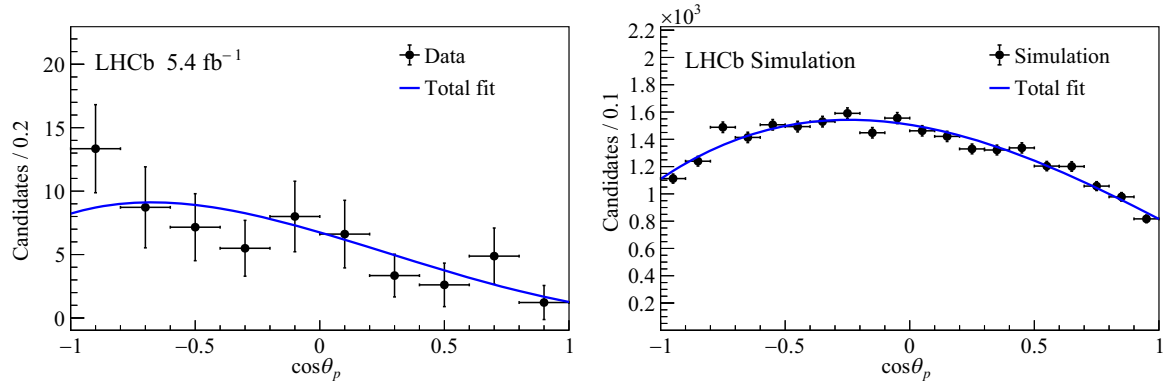

FIG. 3. Distributions of $\cos\theta_p$ in (left) the background-subtracted $B^+ \to p\bar{\Lambda}$ data and (right) the simulated $B^+ \to p\bar{\Lambda}$ sample generated uniformly in phase space, together with the fit results.

TABLE I. Summary of relative systematic uncertainties (in percent) for the measured ratio of branching fractions in the four categories. The total relative uncertainties, obtained by summing all contributions in quadrature, are provided for comparison.

Source	TOS LL	TOS DD	TIS LL	TIS DD
Fit bias	0.3	1.0	2.1	0.9
Fit model	2.9	4.6	4.0	12.4
Simulation sample size	1.1	1.2	1.8	3.1
Data-simulation matching	0.6	1.0	3.3	4.8
Trigger efficiency	2.2	2.2	1.4	1.9
Tracking efficiency	1.0	1.3	1.0	1.4
Kinematic correction	3.5	2.2	0.0	0.5
PID	0.3	0.9	0.5	3.5
$\bar{\Lambda}$ polarization	1.0	0.9	2.1	2.2
K^0_S/Λ branching fraction ratio		1.0		
Total	5.4	6.2	6.4	14.3

quantified using alternative models. As examples, the DSCB function for the signal peak is replaced by a Hypatia function [52], and a second-order Bernstein polynomial is used instead of an exponential function for the combinatorial background. Uncertainties associated with the remaining fit components are found to be negligible.

The statistical uncertainties of the efficiencies due to the finite size of the simulation samples are considered as a source of systematic uncertainty and propagated to the branching fraction ratio. The simulation-based efficiency estimation relies on accurately associating generated and reconstructed particles. The effect of imperfect matching is investigated by redetermining the efficiencies with an alternative method. Furthermore, the hardware-trigger efficiency is calibrated using a data-driven method [53].

Systematic uncertainties associated with the corrections applied to simulation are estimated by using alternative correction schemes or control samples and quantifying the resulting variations in efficiency. The efficiencies could depend on the polarization of the $\bar{\Lambda}$ baryon, which is set to the measured α_B value for the efficiency estimation. Uncertainties related to the $\bar{\Lambda}$ polarization are evaluated by varying the α_B value up and down by one standard deviation and calculating the efficiency shifts.

Among the systematic uncertainties described above, the uncertainties associated with the trigger, tracking, PID efficiency corrections, and $\bar{\Lambda}$ polarization are considered fully correlated across the four data categories due to their reliance on shared calibration sources. All other uncertainties are treated as uncorrelated between different categories. These uncertainties, along with those on the branching fractions of the $\bar{\Lambda} \to \bar{p}\pi^+$ and $K^0_S \to \pi^+\pi^-$ decays, are added in quadrature to give the total systematic uncertainty on the branching fraction ratio $\mathcal{R}$.

Taking into account the correlations of the systematic uncertainties between different data categories, the average result from LHCb Run 2 data is determined to be $\mathcal{R}^{\mathrm{Run2}} = (1.01 \pm 0.14 \pm 0.04) \times 10^{-2}$, which is compatible with the LHCb Run 1 result $\mathcal{R}^{\mathrm{Run1}} = (2.02 \pm 0.88 \pm 0.23) \times 10^{-2}$ [19]. Neglecting the small correlations between the Run 1 and Run 2 results, the combined result is

$$\mathcal{R}^{\mathrm{Run1\&2}} = (1.04 \pm 0.14 \pm 0.04) \times 10^{-2}.$$

Using the known branching fraction $\mathcal{B}(B^+ \to K^0_S\pi^+) = (1.19 \pm 0.03) \times 10^{-5}$ [40], the absolute branching fraction is determined to be

$$\mathcal{B}(B^+ \to p\bar{\Lambda}) = (1.24 \pm 0.17 \pm 0.05 \pm 0.03) \times 10^{-7},$$

where the third uncertainty is due to knowledge of the $B^+ \to K^0_S\pi^+$ branching fraction.

In summary, a search for the rare decay $B^+ \to p\bar{\Lambda}$ is performed using a sample of pp collision data collected at a center-of-mass energy of 13 TeV, corresponding to an integrated luminosity of 5.4 fb^{-1}. An excess of signal candidates over the expected background is observed with a statistical significance exceeding seven standard deviations, when accounting for systematic uncertainties. This represents the first observation of this decay. The measured branching fraction is consistent with available theoretical predictions [20,21] and is more than twenty times lower than that of the $B^+ \to p\bar{\Lambda}\pi^0$ mode [40], supporting the theoretical expectation of threshold enhancement in three-body baryonic B decays. The large value of the measured weak decay parameter α_B indicates a strong interference between the competing S-wave and P-wave amplitudes of the $B^+ \to p\bar{\Lambda}$ decay, which may lead to substantial cancellation between the CP asymmetries of different partial waves.

It is noteworthy that the branching fraction of the $B^+ \to p\bar{\Lambda}$ decay, proceeding via a $\bar{b} \to u\bar{u}\,\bar{s}$ transition, is an order of magnitude higher than that of the $B^0 \to p\bar{p}$ decay [54], which proceeds via a $\bar{b} \to u\bar{u}\,\bar{d}$ transition. This pattern mirrors that in mesonic two-body B-meson decays, where $\bar{b} \to u\bar{u}\,\bar{s}$ transitions (e.g., $B^0_s \to K^+K^-$ and $B^0 \to K^+\pi^-$) dominate over $\bar{b} \to u\bar{u}\,\bar{d}$ transitions (e.g., $B^0_s \to \pi^+K^-$ and $B^0 \to \pi^+\pi^-$). However, this contrasts with the situation in b-baryon decays, where these two types of processes (e.g., $\Lambda^0_b \to pK^-$ and $\Lambda^0_b \to p\pi^-$) exhibit similar branching fractions [40]. These distinctive patterns, in conjunction with the discrepancy in the measured CP violation in $B^0_s \to K^+K^-$, $B^0 \to K^+\pi^-$, and $\Lambda^0_b \to pK^-$ decays, motivate future precision studies. Leveraging the large datasets anticipated from the upgraded LHCb experiment in future running periods, CP violation measurements in the $B^+ \to p\bar{\Lambda}$ decay channel will become feasible, offering a powerful probe into the rich dynamics of heavy-flavor decays and the mechanisms of CP violation.

Acknowledgments—We express our gratitude to our colleagues in the CERN accelerator departments for the excellent performance of the LHC. We thank the technical and administrative staff at the LHCb institutes. We acknowledge support from CERN and from the national agencies: ARC (Australia); CAPES, CNPq, FAPERJ, and FINEP (Brazil); MOST and NSFC (China); CNRS/IN2P3 (France); BMFTR, DFG, and MPG (Germany); INFN (Italy); NWO (Netherlands); MNiSW and NCN (Poland); MCID/IFA (Romania); MICIU and AEI (Spain); SNSF and SER (Switzerland); NASU (Ukraine); STFC (United Kingdom); DOE NP and NSF (USA). We acknowledge the computing resources that are provided by ARDC (Australia), CBPF (Brazil), CERN, IHEP and LZU (China), IN2P3 (France), KIT and DESY (Germany), INFN (Italy), SURF (Netherlands), Polish WLCG (Poland), IFIN-HH (Romania), PIC (Spain), CSCS (Switzerland), and GridPP (United Kingdom). We are indebted to the communities behind the multiple open-source software packages on which we depend. Individual groups or members have received support from Key Research Program of Frontier Sciences of CAS, CAS PIFI, CAS CCEPP, Minciencias (Colombia); EPLANET, Marie Skłodowska-Curie Actions, ERC, and NextGenerationEU (European Union); A*MIDEX, ANR, IPhU and Labex P2IO, and Région Auvergne-Rhône-Alpes (France); Alexander-von-Humboldt Foundation (Germany); ICSC (Italy); Severo Ochoa and María de Maeztu Units of Excellence, GVA, XuntaGal, GENCAT, InTalent-Inditex, and Prog. Atracción Talento CM (Spain); SRC (Sweden); the Leverhulme Trust, the Royal Society, and UKRI (United Kingdom).

Data availability—The data that support the findings of this article are openly available [55].

[1] B. Aubert *et al.* (*BABAR* Collaboration), Study of $B^0 \to \pi^0\pi^0$, $B^\pm \to \pi^\pm\pi^0$, and $B^\pm \to K^\pm\pi^0$ decays, and isospin analysis of $B \to \pi\pi$ decays, Phys. Rev. D **76**, 091102 (2007).

[2] B. Aubert *et al.* (*BABAR* Collaboration), Measurement of the *CP*-violating asymmetries in $B^0 \to K^0_S\pi^0$ and of the branching fraction $B^0 \to K^0\pi^0$, Phys. Rev. D **77**, 012003 (2008).

[3] B. Aubert *et al.* (*BABAR* Collaboration), Observation of *CP* violation in $B^0 \to K^+\pi^-$ and $B^0 \to \pi^+\pi^-$, Phys. Rev. Lett. **99**, 021603 (2007).

[4] J. P. Lees *et al.* (*BABAR* Collaboration), Measurement of *CP* asymmetries and branching fractions in charmless two-body *B*-meson decays to pions and kaons, Phys. Rev. D **87**, 052009 (2013).

[5] S.-W. Lin *et al.* (Belle Collaboration), Measurements of branching fractions for $B \to K\pi$ and $B \to \pi\pi$ decays, Phys. Rev. Lett. **99**, 121601 (2007).

[6] H. Ishino *et al.* (Belle Collaboration), Observation of direct CP-violation in $B^0 \to \pi^+\pi^-$ decays and model-independent constraints on the quark-mixing angle ϕ_2, Phys. Rev. Lett. **98**, 211801 (2007).

[7] S.-W. Lin *et al.* (Belle Collaboration), Observation of B decays to two kaons, Phys. Rev. Lett. **98**, 181804 (2007).

[8] M. Fujikawa *et al.* (Belle Collaboration), Measurement of CP asymmetries in $B^0 \to K^0\pi^0$ decays, Phys. Rev. D **81**, 011101 (2010).

[9] R. Aaij *et al.* (LHCb Collaboration), Observation of the $B^0_s \to \eta'\eta'$ decay, Phys. Rev. Lett. **115**, 051801 (2015).

[10] R. Aaij *et al.* (LHCb Collaboration), Observation of the annihilation decay mode $B^0 \to K^+K^-$, Phys. Rev. Lett. **118**, 081801 (2017).

[11] R. Aaij *et al.* (LHCb Collaboration), Measurement of *CP* asymmetries in two-body $B^0_{(s)}$-meson decays to charged pions and kaons, Phys. Rev. D **98**, 032004 (2018).

[12] R. Aaij *et al.* (LHCb Collaboration), Measurement of the branching fraction of the decay $B^0_s \to K^0_S K^0_S$, Phys. Rev. D **102**, 012011 (2020).

[13] R. Aaij *et al.* (LHCb Collaboration), Observation of *CP* violation in two-body $B^0_{(s)}$-meson decays to charged pions and kaons, J. High Energy Phys. 03 (2021) 075.

[14] R. Aaij *et al.* (LHCb Collaboration), Measurement of *CP* violation in the decay $B^+ \to K^+\pi^0$, Phys. Rev. Lett. **126**, 091802 (2021).

[15] R. Aaij *et al.* (LHCb Collaboration), First observation of the rare purely baryonic decay $B^0 \to p\bar{p}$, Phys. Rev. Lett. **119**, 232001 (2017).

[16] R. Aaij *et al.* (LHCb Collaboration), Studies of the decays $B^+ \to p\bar{p}h^+$ and observation of $B^+ \to \bar{\Lambda}(1520)p$, Phys. Rev. D **88**, 052015 (2013).

[17] T. E. Coan *et al.* (CLEO Collaboration), Search for exclusive rare baryonic decays of B mesons, Phys. Rev. D **59**, 111101 (1999).

[18] Y.-T. Tsai *et al.* (Belle Collaboration), Search for $B^0 \to p\bar{p}, \Lambda\bar{\Lambda}$ and $B^+ \to p\bar{\Lambda}$ at Belle, Phys. Rev. D **75**, 111101 (2007).

[19] R. Aaij *et al.* (LHCb Collaboration), Evidence for the two-body charmless baryonic decay $B^+ \to p\bar{\Lambda}$, J. High Energy Phys. 04 (2017) 162.

[20] H.-Y. Cheng and K.-C. Yang, Charmless exclusive baryonic B decays, Phys. Rev. D **66**, 014020 (2002).

[21] C.-K. Chua, Charmless two-body baryonic $B_{u,d,s}$ decays revisited, Phys. Rev. D **89**, 056003 (2014).

[22] C.-K. Chua, Rates and CP asymmetries of charmless two-body baryonic $B_{u,d,s}$ decays, Phys. Rev. D **95**, 096004 (2017).

[23] X. Huang, Y.-K. Hsiao, J. Wang, and L. Sun, Baryonic *B* meson decays, Adv. High Energy Phys. **2022**, 4343824 (2022).

[24] Y. K. Hsiao and C. Q. Geng, Violation of partial conservation of the axial-vector current and two-body baryonic *B* and D_s decays, Phys. Rev. D **91**, 077501 (2015).

[25] H.-Y. Cheng and C.-K. Chua, Smallness of tree-dominated charmless two-body baryonic *B* decay rates, Phys. Rev. D **91**, 036003 (2015).

[26] J.-J. Han, J.-X. Yu, Y. Li, H.-n. Li, J.-P. Wang, Z.-J. Xiao, and F.-S. Yu, Establishing CP violation in b-baryon decays, Phys. Rev. Lett. **134**, 221801 (2025).

[27] R. Aaij *et al.* (LHCb Collaboration), Measurement of *CP* asymmetries in $\Lambda_b^0 \to ph^-$ decays, Phys. Rev. D **111**, 092004 (2025).
[28] J.-J. Han *et al.*, CP violation in two-body hadronic Λ_b decays in the PQCD approach, Phys. Rev. D **112**, 053007 (2025).
[29] C.-Q. Geng, X.-N. Jin, and C.-W. Liu, CP asymmetries in B meson two-body baryonic decays, Phys. Lett. B **846**, 138240 (2023).
[30] A. A. Alves, Jr. *et al.* (LHCb Collaboration), The LHCb detector at the LHC, J. Instrum. **3**, S08005 (2008).
[31] LHCb Collaboration, LHCb detector performance, Int. J. Mod. Phys. A **30**, 1530022 (2015).
[32] T. Sjöstrand, S. Mrenna, and P. Skands, A brief introduction to PYTHIA 8.1, Comput. Phys. Commun. **178**, 852 (2008); PYTHIA 6.4 physics and manual, J. High Energy Phys. 05 (2006) 026.
[33] D. J. Lange, The EvtGen particle decay simulation package, Nucl. Instrum. Methods Phys. Res., Sect. A **462**, 152 (2001).
[34] P. Golonka and Z. Was, PHOTOS Monte Carlo: A precision tool for QED corrections in Z and W decays, Eur. Phys. J. C **45**, 97 (2006).
[35] J. Allison *et al.* (Geant4 Collaboration), Geant4 developments and applications, IEEE Trans. Nucl. Sci. **53**, 270 (2006); S. Agostinelli *et al.* (Geant4 Collaboration), Geant4: A simulation toolkit, Nucl. Instrum. Methods Phys. Res., Sect. A **506**, 250 (2003).
[36] M. Clemencic, G. Corti, S. Easo, C. R. Jones, S. Miglioranzi, M. Pappagallo, and P. Robbe, The LHCb simulation application, Gauss: Design, evolution and experience, J. Phys. Conf. Ser. **331**, 032023 (2011).
[37] R. Aaij *et al.*, Selection and processing of calibration samples to measure the particle identification performance of the LHCb experiment in Run 2, Eur. Phys. J. Tech. Instrum. **6**, 1 (2019).
[38] R. Aaij *et al.*, Design and performance of the LHCb trigger and full real-time reconstruction in Run 2 of the LHC, J. Instrum. **14**, P04013 (2019).
[39] R. Aaij *et al.*, The LHCb trigger and its performance in 2011, J. Instrum. **8**, P04022 (2013).
[40] S. Navas *et al.* (Particle Data Group), Review of particle physics, Phys. Rev. D **110**, 030001 (2024).
[41] L. Breiman, J. H. Friedman, R. A. Olshen, and C. J. Stone, *Classification and Regression Trees* (Wadsworth International Group, Belmont, California, USA, 1984).
[42] Y. Freund and R. E. Schapire, A decision-theoretic generalization of on-line learning and an application to boosting, J. Comput. Syst. Sci. **55**, 119 (1997).
[43] G. Punzi, Sensitivity of searches for new signals and its optimization, eConf C **030908**, MODT002 (2003), https://www.slac.stanford.edu/econf/C030908/.
[44] T. Skwarnicki, A study of the radiative cascade transitions between the upsilon-prime and upsilon resonances, Ph.D. thesis, Institute of Nuclear Physics, Krakow, 1986; DESY-F31-86-02.
[45] K. Cranmer, Kernel estimation in high-energy physics, Comput. Phys. Commun. **136**, 198 (2001).
[46] H. Albrecht *et al.* (ARGUS Collaboration), Search for hadronic $b \to u$ decays, Phys. Lett. B **241**, 278 (1990).
[47] S. S. Wilks, The large-sample distribution of the likelihood ratio for testing composite hypotheses, Ann. Math. Stat. **9**, 60 (1938).
[48] M. Pivk and F. R. Le Diberder, sPlot: A statistical tool to unfold data distributions, Nucl. Instrum. Methods Phys. Res., Sect. A **555**, 356 (2005).
[49] M. Jacob and G. C. Wick, On the general theory of collisions for particles with spin, Ann. Phys. (N.Y.) **7**, 404 (1959).
[50] M. Ablikim *et al.* (BESIII Collaboration), Precise measurements of decay parameters and *CP* asymmetry with entangled $\Lambda - \bar{\Lambda}$ pairs, Phys. Rev. Lett. **129**, 131801 (2022).
[51] Y. Xie, sFit: A method for background subtraction in maximum likelihood fit, arXiv:0905.0724.
[52] D. Martínez Santos and F. Dupertuis, Mass distributions marginalized over per-event errors, Nucl. Instrum. Methods Phys. Res., Sect. A **764**, 150 (2014).
[53] A. Martin Sanchez, P. Robbe, and M.-H. Schune, Performances of the LHCb L0 calorimeter trigger, Reports No. LHCb-PUB-2011-026, No. CERN-LHCb-PUB-2011-026, CERN, Geneva, 2012.
[54] R. Aaij *et al.* (LHCb Collaboration), Search for the rare hadronic decay $B_s^0 \to p\bar{p}$, Phys. Rev. D **108**, 012007 (2023).
[55] https://cds.cern.ch/record/2950031.

End Matter

Additional mass fit and angular fit results—The obtained yields of $B^+ \to p\bar{\Lambda}$ and $B^+ \to K_S^0\pi^+$ decays in different data categories are given in Table II. The profile-likelihood scans of the baseline mass fit and angular fit, including the effects of systematic uncertainties, are shown in Fig. 4.

TABLE II. Branching fraction ratio $\mathcal{R}$ calculated in four data categories. The efficiency ratio is determined from simulation, and the yields are obtained from the baseline fit results. The first uncertainty on $\mathcal{R}$ is statistical, and the second is systematic.

Parameter	TOS LL	TOS DD	TIS LL	TIS DD
$N(K^0_S\pi^+)$	$12\,200 \pm 140$	9250 ± 130	5570 ± 100	1480 ± 50
$N(p\bar{\Lambda})$	40 ± 8	26 ± 6	17 ± 5	5 ± 4
$[\epsilon(K^0_S\pi^+)/\epsilon(p\bar{\Lambda})]$	2.62 ± 0.14	3.62 ± 0.18	3.57 ± 0.21	2.66 ± 0.24
$\mathcal{R}(10^{-2})$	$0.93 \pm 0.19 \pm 0.05$	$1.11 \pm 0.28 \pm 0.07$	$1.18 \pm 0.38 \pm 0.08$	$0.95 \pm 0.82 \pm 0.14$
		$1.04 \pm 0.14 \pm 0.04$		

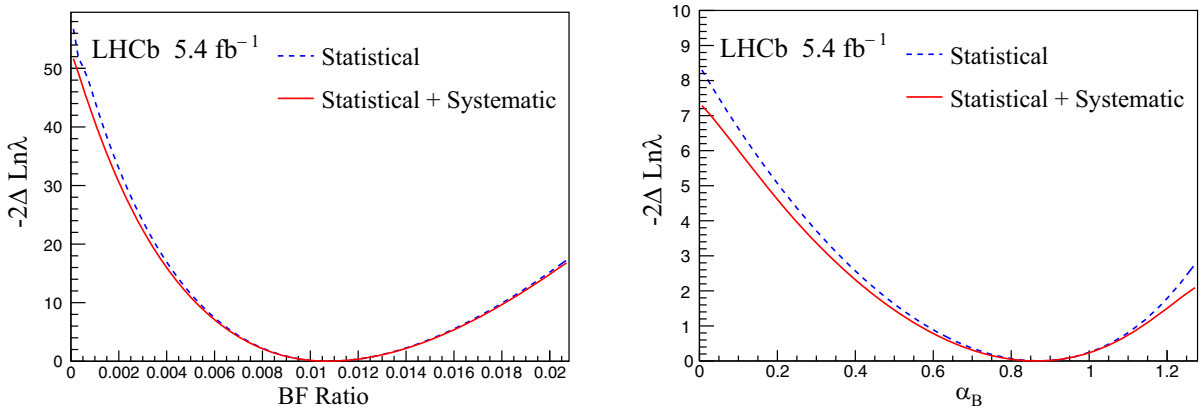

FIG. 4. Profile-likelihood scan curves for (left) the mass fit and (right) the angular fit. Blue curves show results with statistical uncertainties only, while red curves include the effect of systematic uncertainties, incorporated via convolution with a Gaussian distribution.

R. Aaij,[38] A. S. W. Abdelmotteleb,[58] C. Abellan Beteta,[52] F. Abudinén,[58] T. Ackernley,[62] A. A. Adefisoye,[70] B. Adeva,[48] M. Adinolfi,[56] P. Adlarson,[86] C. Agapopoulou,[14] C. A. Aidala,[88] Z. Ajaltouni,[11] S. Akar,[11] K. Akiba,[38] P. Albicocco,[28] J. Albrecht,[19,a] R. Aleksiejunas,[82] F. Alessio,[50] P. Alvarez Cartelle,[57] R. Amalric,[16] S. Amato,[3] J. L. Amey,[56] Y. Amhis,[14] L. An,[6] L. Anderlini,[27] M. Andersson,[52] P. Andreola,[52] M. Andreotti,[26] S. Andres Estrada,[45] A. Anelli,[31,50,b] D. Ao,[7] C. Arata,[12] F. Archilli,[37,c] Z. Areg,[70] M. Argenton,[26] S. Arguedas Cuendis,[9,50] L. Arnone,[31,b] A. Artamonov,[44] M. Artuso,[70] E. Aslanides,[13] R. Ataíde Da Silva,[51] M. Atzeni,[66] B. Audurier,[12] J. A. Authier,[15] D. Bacher,[65] I. Bachiller Perea,[51] S. Bachmann,[22] M. Bachmayer,[51] J. J. Back,[58] P. Baladron Rodriguez,[48] V. Balagura,[15] A. Balboni,[26] W. Baldini,[26] Z. Baldwin,[80] L. Balzani,[19] H. Bao,[7] J. Baptista de Souza Leite,[2] C. Barbero Pretel,[48,12] M. Barbetti,[27] I. R. Barbosa,[71] R. J. Barlow,[64] M. Barnyakov,[25] S. Barsuk,[14] W. Barter,[60] J. Bartz,[70] S. Bashir,[40] B. Batsukh,[5] P. B. Battista,[14] A. Bay,[51] A. Beck,[66] M. Becker,[19] F. Bedeschi,[35] I. B. Bediaga,[2] N. A. Behling,[19] S. Belin,[48] A. Bellavista,[25] K. Belous,[44] I. Belov,[29] I. Belyaev,[36] G. Benane,[13] G. Bencivenni,[28] E. Ben-Haim,[16] A. Berezhnoy,[44] R. Bernet,[52] S. Bernet Andres,[47] A. Bertolin,[33] F. Betti,[60] J. Bex,[57] O. Bezshyyko,[87] S. Bhattacharya,[81] J. Bhom,[41] M. S. Bieker,[18] N. V. Biesuz,[26] A. Biolchini,[38] M. Birch,[63] F. C. R. Bishop,[10] A. Bitadze,[64] A. Bizzeti,[27,d] T. Blake,[58,e] F. Blanc,[51] J. E. Blank,[19] S. Blusk,[70] V. Bocharnikov,[44] J. A. Boelhauve,[19] O. Boente Garcia,[50] T. Boettcher,[69] A. Bohare,[60] A. Boldyrev,[44] C. Bolognani,[84] R. Bolzonella,[26,f] R. B. Bonacci,[1] N. Bondar,[44,50] A. Bordelius,[50] F. Borgato,[33,50] S. Borghi,[64] M. Borsato,[31,b] J. T. Borsuk,[85] E. Bottalico,[62] S. A. Bouchiba,[51] M. Bovill,[65] T. J. V. Bowcock,[62] A. Boyer,[50] C. Bozzi,[26] J. D. Brandenburg,[89]

A. Brea Rodriguez,[51] N. Breer,[19] J. Brodzicka,[41] J. Brown,[62] D. Brundu,[32] E. Buchanan,[60] M. Burgos Marcos,[84] A. T. Burke,[64] C. Burr,[50] C. Buti,[27] J. S. Butter,[57] J. Buytaert,[50] W. Byczynski,[50] S. Cadeddu,[32] H. Cai,[76] Y. Cai,[5] A. Caillet,[16] R. Calabrese,[26,f] S. Calderon Ramirez,[9] L. Calefice,[46] M. Calvi,[31,b] M. Calvo Gomez,[47] P. Camargo Magalhaes,[2,g] J. I. Cambon Bouzas,[48] P. Campana,[28] A. F. Campoverde Quezada,[7] S. Capelli,[31] M. Caporale,[25] L. Capriotti,[26] R. Caravaca-Mora,[9] A. Carbone,[25,h] L. Carcedo Salgado,[48] R. Cardinale,[29,i] A. Cardini,[32] P. Carniti,[31] L. Carus,[22] A. Casais Vidal,[66] R. Caspary,[22] G. Casse,[62] M. Cattaneo,[50] G. Cavallero,[26] V. Cavallini,[26,f] S. Celani,[50] I. Celestino,[35,j] S. Cesare,[30,k] A. J. Chadwick,[62] I. Chahrour,[88] H. Chang,[4,l] M. Charles,[16] Ph. Charpentier,[50] E. Chatzianagnostou,[38] R. Cheaib,[81] M. Chefdeville,[10] C. Chen,[57] J. Chen,[51] S. Chen,[5] Z. Chen,[7] A. Chen Hu,[63] M. Cherif,[12] A. Chernov,[41] S. Chernyshenko,[54] X. Chiotopoulos,[84] V. Chobanova,[45] M. Chrzaszcz,[41] A. Chubykin,[44] V. Chulikov,[28,36,50] P. Ciambrone,[28] X. Cid Vidal,[48] G. Ciezarek,[50] P. Cifra,[38] P. E. L. Clarke,[60] M. Clemencic,[50] H. V. Cliff,[57] J. Closier,[50] C. Cocha Toapaxi,[22] V. Coco,[50] J. Cogan,[13] E. Cogneras,[11] L. Cojocariu,[43] S. Collaviti,[51] P. Collins,[50] T. Colombo,[50] M. Colonna,[19] A. Comerma-Montells,[46] L. Congedo,[24] J. Connaughton,[58] A. Contu,[32] N. Cooke,[61] G. Cordova,[35,j] C. Coronel,[67] I. Corredoira,[12] A. Correia,[16] G. Corti,[50] J. Cottee Meldrum,[56] B. Couturier,[50] D. C. Craik,[52] M. Cruz Torres,[2,m] E. Curras Rivera,[51] R. Currie,[60] C. L. Da Silva,[69] S. Dadabaev,[44] X. Dai,[4] E. Dall'Occo,[50] J. Dalseno,[45] C. D'Ambrosio,[63] J. Daniel,[11] G. Darze,[3] A. Davidson,[58] J. E. Davies,[64] O. De Aguiar Francisco,[64] C. De Angelis,[32,n] F. De Benedetti,[50] J. de Boer,[38] K. De Bruyn,[83] S. De Capua,[64] M. De Cian,[64,50] U. De Freitas Carneiro Da Graca,[2,o] E. De Lucia,[28] J. M. De Miranda,[2] L. De Paula,[3] M. De Serio,[24,p] P. De Simone,[28] F. De Vellis,[19] J. A. de Vries,[84] F. Debernardis,[24] D. Decamp,[10] S. Dekkers,[1] L. Del Buono,[16] B. Delaney,[66] H.-P. Dembinski,[19] J. Deng,[8] V. Denysenko,[52] O. Deschamps,[11] F. Dettori,[32,n] B. Dey,[81] P. Di Nezza,[28] I. Diachkov,[44] S. Didenko,[44] S. Ding,[70] Y. Ding,[51] L. Dittmann,[22] V. Dobishuk,[54] A. D. Docheva,[61] A. Doheny,[58] C. Dong,[4,l] A. M. Donohoe,[23] F. Dordei,[32] A. C. dos Reis,[2] A. D. Dowling,[70] L. Dreyfus,[13] W. Duan,[74] P. Duda,[85] L. Dufour,[50] V. Duk,[34] P. Durante,[50] M. M. Duras,[85] J. M. Durham,[69] O. D. Durmus,[81] A. Dziurda,[41] A. Dzyuba,[44] S. Easo,[59] E. Eckstein,[18] U. Egede,[1] A. Egorychev,[44] V. Egorychev,[44] S. Eisenhardt,[60] E. Ejopu,[62] L. Eklund,[86] M. Elashri,[67] D. Elizondo Blanco,[9] J. Ellbracht,[19] S. Ely,[63] A. Ene,[43] J. Eschle,[70] S. Esen,[22] T. Evans,[38] F. Fabiano,[32] S. Faghih,[67] L. N. Falcao,[31,b] B. Fang,[7] R. Fantechi,[35] L. Fantini,[34,q] M. Faria,[51] K. Farmer,[60] F. Fassin,[83,38] D. Fazzini,[31,b] L. Felkowski,[85] M. Feng,[5,7] A. Fernandez Casani,[49] M. Fernandez Gomez,[48] A. D. Fernez,[68] F. Ferrari,[25,h] F. Ferreira Rodrigues,[3] M. Ferrillo,[52] M. Ferro-Luzzi,[50] S. Filippov,[44] R. A. Fini,[24] M. Fiorini,[26,f] M. Firlej,[40] K. L. Fischer,[65] D. S. Fitzgerald,[88] C. Fitzpatrick,[64] T. Fiutowski,[40] F. Fleuret,[15] A. Fomin,[53] M. Fontana,[25] L. A. Foreman,[64] R. Forty,[50] D. Foulds-Holt,[60] V. Franco Lima,[3] M. Franco Sevilla,[68] M. Frank,[50] E. Franzoso,[26,f] G. Frau,[64] C. Frei,[50] D. A. Friday,[64,50] J. Fu,[7] Q. Führing,[19,57,a] T. Fulghesu,[13] G. Galati,[24] M. D. Galati,[38] A. Gallas Torreira,[48] D. Galli,[25,h] S. Gambetta,[60] M. Gandelman,[3] P. Gandini,[30] B. Ganie,[64] H. Gao,[7] R. Gao,[65] T. Q. Gao,[57] Y. Gao,[8] Y. Gao,[6] Y. Gao,[8] L. M. Garcia Martin,[51] P. Garcia Moreno,[46] J. García Pardiñas,[66] P. Gardner,[68] L. Garrido,[46] C. Gaspar,[50] A. Gavrikov,[33] L. L. Gerken,[19] E. Gersabeck,[20] M. Gersabeck,[20] T. Gershon,[58] S. Ghizzo,[29,i] Z. Ghorbanimoghaddam,[56] F. I. Giasemis,[16,r] V. Gibson,[57] H. K. Giemza,[42] A. L. Gilman,[67] M. Giovannetti,[28] A. Gioventù,[46] L. Girardey,[64,59] M. A. Giza,[41] F. C. Glaser,[14,22] V. V. Gligorov,[16] C. Göbel,[71] L. Golinka-Bezshyyko,[87] E. Golobardes,[47] D. Golubkov,[44] A. Golutvin,[63,50] S. Gomez Fernandez,[46] W. Gomulka,[40] I. Gonçales Vaz,[50] F. Goncalves Abrantes,[65] M. Goncerz,[41] G. Gong,[4,l] J. A. Gooding,[19] I. V. Gorelov,[44] C. Gotti,[31] E. Govorkova,[66] J. P. Grabowski,[30] L. A. Granado Cardoso,[50] E. Graugés,[46] E. Graverini,[51,s] L. Grazette,[58] G. Graziani,[27] A. T. Grecu,[43] N. A. Grieser,[67] L. Grillo,[61] S. Gromov,[44] C. Gu,[15] M. Guarise,[26] L. Guerry,[11] A.-K. Guseinov,[51] E. Gushchin,[44] Y. Guz,[6,50] T. Gys,[50] K. Habermann,[18] T. Hadavizadeh,[1] C. Hadjivasiliou,[68] G. Haefeli,[51] C. Haen,[50] S. Haken,[57] G. Hallett,[58] P. M. Hamilton,[68] J. Hammerich,[62] Q. Han,[33] X. Han,[22,50] S. Hansmann-Menzemer,[22] L. Hao,[7] N. Harnew,[65] T. H. Harris,[1] M. Hartmann,[14] S. Hashmi,[40] J. He,[7,t] N. Heatley,[14] A. Hedes,[64] F. Hemmer,[50] C. Henderson,[67] R. Henderson,[14] R. D. L. Henderson,[1] A. M. Hennequin,[50] K. Hennessy,[62] L. Henry,[51] J. Herd,[63] P. Herrero Gascon,[22] J. Heuel,[17] A. Heyn,[13] A. Hicheur,[3] G. Hijano Mendizabal,[52] J. Horswill,[64] R. Hou,[8] Y. Hou,[11] D. C. Houston,[61] N. Howarth,[62] W. Hu,[7] X. Hu,[4] W. Hulsbergen,[38] R. J. Hunter,[58] M. Hushchyn,[44]

D. Hutchcroft,[62] M. Idzik,[40] D. Ilin,[44] P. Ilten,[67] A. Iniukhin,[44] A. Iohner,[10] A. Ishteev,[44] K. Ivshin,[44] H. Jage,[17] S. J. Jaimes Elles,[78,49,50] S. Jakobsen,[50] T. Jakoubek,[79] E. Jans,[38] B. K. Jashal,[49] A. Jawahery,[68] C. Jayaweera,[55] V. Jevtic,[19] Z. Jia,[16] E. Jiang,[68] X. Jiang,[5,7] Y. Jiang,[7] Y. J. Jiang,[6] E. Jimenez Moya,[9] N. Jindal,[89] M. John,[65] A. John Rubesh Rajan,[23] D. Johnson,[55] C. R. Jones,[57] S. Joshi,[42] B. Jost,[50] J. Juan Castella,[57] N. Jurik,[50] I. Juszczak,[41] K. Kalecinska,[40] D. Kaminaris,[51] S. Kandybei,[53] M. Kane,[60] Y. Kang,[4,l] C. Kar,[11] M. Karacson,[50] A. Kauniskangas,[51] J. W. Kautz,[67] M. K. Kazanecki,[41] F. Keizer,[50] M. Kenzie,[57] T. Ketel,[38] B. Khanji,[70] A. Kharisova,[44] S. Kholodenko,[63,50] G. Khreich,[14] T. Kirn,[17] V. S. Kirsebom,[31,b] O. Kitouni,[66] S. Klaver,[39] N. Kleijne,[35,j] A. Kleimenova,[51] D. K. Klekots,[87] K. Klimaszewski,[42] M. R. Kmiec,[42] T. Knospe,[19] R. Kolb,[22] S. Koliiev,[54] L. Kolk,[19] A. Konoplyannikov,[6] P. Kopciewicz,[50] P. Koppenburg,[38] A. Korchin,[53] M. Korolev,[44] I. Kostiuk,[38] O. Kot,[54] S. Kotriakhova, E. Kowalczyk,[68] A. Kozachuk,[44] P. Kravchenko,[44] L. Kravchuk,[44] O. Kravcov,[82] M. Kreps,[58] P. Krokovny,[44] W. Krupa,[70] W. Krzemien,[42] O. Kshyvanskyi,[54] S. Kubis,[85] M. Kucharczyk,[41] V. Kudryavtsev,[44] E. Kulikova,[44] A. Kupsc,[86] V. Kushnir,[53] B. Kutsenko,[13] J. Kvapil,[69] I. Kyryllin,[53] D. Lacarrere,[50] P. Laguarta Gonzalez,[46] A. Lai,[32] A. Lampis,[32] D. Lancierini,[63] C. Landesa Gomez,[48] J. J. Lane,[1] G. Lanfranchi,[28] C. Langenbruch,[22] J. Langer,[19] T. Latham,[58] F. Lazzari,[35,50,s] C. Lazzeroni,[55] R. Le Gac,[13] H. Lee,[62] R. Lefèvre,[11] A. Leflat,[44] S. Legotin,[44] M. Lehuraux,[58] E. Lemos Cid,[50] O. Leroy,[13] T. Lesiak,[41] E. D. Lesser,[50] B. Leverington,[22] A. Li,[4,l] C. Li,[4,l] C. Li,[13] H. Li,[74] J. Li,[8] K. Li,[77] L. Li,[64] M. Li,[8] P. Li,[7] P.-R. Li,[75] Q. Li,[5,7] T. Li,[73] T. Li,[74] Y. Li,[8] Y. Li,[5] Y. Li,[4] Z. Lian,[4,l] Q. Liang,[8] X. Liang,[70] Z. Liang,[32] S. Libralon,[49] A. Lightbody,[12] C. Lin,[7] T. Lin,[59] R. Lindner,[50] H. Linton,[63] R. Litvinov,[32] D. Liu,[8] F. L. Liu,[1] G. Liu,[74] K. Liu,[75] S. Liu,[5] W. Liu,[8] Y. Liu,[60] Y. Liu,[75] Y. L. Liu,[63] G. Loachamin Ordonez,[71] I. Lobo,[1] A. Lobo Salvia,[46] A. Loi,[32] T. Long,[57] F. C. L. Lopes,[2,g] J. H. Lopes,[3] A. Lopez Huertas,[46] C. Lopez Iribarnegaray,[48] S. López Soliño,[48] Q. Lu,[15] C. Lucarelli,[50] D. Lucchesi,[33,u] M. Lucio Martinez,[49] Y. Luo,[6] A. Lupato,[33,v] E. Luppi,[26,f] K. Lynch,[23] X.-R. Lyu,[7] G. M. Ma,[4,l] H. Ma,[73] S. Maccolini,[19] F. Machefert,[14] F. Maciuc,[43] B. Mack,[70] I. Mackay,[65] L. M. Mackey,[70] L. R. Madhan Mohan,[57] M. J. Madurai,[55] D. Magdalinski,[38] D. Maisuzenko,[44] J. J. Malczewski,[41] S. Malde,[65] L. Malentacca,[50] A. Malinin,[44] T. Maltsev,[44] G. Manca,[32,n] G. Mancinelli,[13] C. Mancuso,[14] R. Manera Escalero,[46] F. M. Manganella,[37] D. Manuzzi,[25] D. Marangotto,[30,k] J. F. Marchand,[10] R. Marchevski,[51] U. Marconi,[25] E. Mariani,[16] S. Mariani,[50] C. Marin Benito,[46] J. Marks,[22] A. M. Marshall,[56] L. Martel,[65] G. Martelli,[34] G. Martellotti,[36] L. Martinazzoli,[50] M. Martinelli,[31,b] D. Martinez Gomez,[83] D. Martinez Santos,[45] F. Martinez Vidal,[49] A. Martorell i Granollers,[47] A. Massafferri,[2] R. Matev,[50] A. Mathad,[50] V. Matiunin,[44] C. Matteuzzi,[70] K. R. Mattioli,[15] A. Mauri,[63] E. Maurice,[15] J. Mauricio,[46] P. Mayencourt,[51] J. Mazorra de Cos,[49] M. Mazurek,[42] M. McCann,[63] N. T. McHugh,[61] A. McNab,[64] R. McNulty,[23] B. Meadows,[67] G. Meier,[19] D. Melnychuk,[42] D. Mendoza Granada,[16] P. Menendez Valdes Perez,[48] F. M. Meng,[4,l] M. Merk,[38,84] A. Merli,[51,30] L. Meyer Garcia,[68] D. Miao,[5,7] H. Miao,[7] M. Mikhasenko,[80] D. A. Milanes,[78,w] A. Minotti,[31,b] E. Minucci,[28] T. Miralles,[11] B. Mitreska,[64] D. S. Mitzel,[19] R. Mocanu,[43] A. Modak,[59] L. Moeser,[19] R. D. Moise,[17] E. F. Molina Cardenas,[88] T. Mombächer,[67] M. Monk,[57] S. Monteil,[11] A. Morcillo Gomez,[48] G. Morello,[28] M. J. Morello,[35,j] M. P. Morgenthaler,[22] A. Moro,[31,b] J. Moron,[40] W. Morren,[38] A. B. Morris,[50] A. G. Morris,[13] R. Mountain,[70] Z. M. Mu,[6] E. Muhammad,[58] F. Muheim,[60] M. Mulder,[83] K. Müller,[52] F. Muñoz-Rojas,[9] R. Murta,[63] V. Mytrochenko,[53] P. Naik,[62] T. Nakada,[51] R. Nandakumar,[59] T. Nanut,[50] I. Nasteva,[3] M. Needham,[60] E. Nekrasova,[44] N. Neri,[30,k] S. Neubert,[18] N. Neufeld,[50] P. Neustroev,[44] J. Nicolini,[50] D. Nicotra,[84] E. M. Niel,[15] N. Nikitin,[44] L. Nisi,[19] Q. Niu,[75] P. Nogarolli,[3] P. Nogga,[18] C. Normand,[56] J. Novoa Fernandez,[48] G. Nowak,[67] C. Nunez,[88] H. N. Nur,[61] A. Oblakowska-Mucha,[40] V. Obraztsov,[44] T. Oeser,[17] A. Okhotnikov,[44] O. Okhrimenko,[54] R. Oldeman,[32,n] F. Oliva,[60,50] E. Olivart Pino,[46] M. Olocco,[19] R. H. O'Neil,[50] J. S. Ordonez Soto,[11] D. Osthues,[19] J. M. Otalora Goicochea,[3] P. Owen,[52] A. Oyanguren,[49] O. Ozcelik,[50] F. Paciolla,[35,x] A. Padee,[42] K. O. Padeken,[18] B. Pagare,[48] T. Pajero,[50] A. Palano,[24] L. Palini,[30] M. Palutan,[28] C. Pan,[76] X. Pan,[4,l] S. Panebianco,[12] S. Paniskaki,[50,33] G. Panshin,[5] L. Paolucci,[64] A. Papanestis,[59] M. Pappagallo,[24,p] L. L. Pappalardo,[26] C. Pappenheimer,[67] C. Parkes,[64] D. Parmar,[80] G. Passaleva,[27] D. Passaro,[35,50,j] A. Pastore,[24] M. Patel,[63] J. Patoc,[65] C. Patrignani,[25,h] A. Paul,[70] C. J. Pawley,[84] A. Pellegrino,[38] J. Peng,[5,7] X. Peng,[75] M. Pepe Altarelli,[28] S. Perazzini,[25] D. Pereima,[44] H. Pereira Da Costa,[69] M. Pereira Martinez,[48]

A. Pereiro Castro,[48] C. Perez,[47] P. Perret,[11] A. Perrevoort,[83] A. Perro,[50,13] M. J. Peters,[67] K. Petridis,[56] A. Petrolini,[29,i] S. Pezzulo,[29,i] J. P. Pfaller,[67] H. Pham,[70] L. Pica,[35,j] M. Piccini,[34] L. Piccolo,[32] B. Pietrzyk,[10] G. Pietrzyk,[14] R. N. Pilato,[62] D. Pinci,[36] F. Pisani,[50] M. Pizzichemi,[31,50,b] V. M. Placinta,[43] M. Plo Casasus,[48] T. Poeschl,[50] F. Polci,[16] M. Poli Lener,[28] A. Poluektov,[13] N. Polukhina,[44] I. Polyakov,[64] E. Polycarpo,[3] S. Ponce,[50] D. Popov,[7,50] K. Popp,[19] S. Poslavskii,[44] K. Prasanth,[60] C. Prouve,[45] D. Provenzano,[32,50,n] V. Pugatch,[54] A. Puicercus Gomez,[50] G. Punzi,[35,s] J. R. Pybus,[69] Q. Q. Qian,[6] W. Qian,[7] N. Qin,[4,l] R. Quagliani,[50] R. I. Rabadan Trejo,[58] R. Racz,[82] J. H. Rademacker,[56] M. Rama,[35] M. Ramírez García,[88] V. Ramos De Oliveira,[71] M. Ramos Pernas,[58] M. S. Rangel,[3] F. Ratnikov,[44] G. Raven,[39] M. Rebollo De Miguel,[49] F. Redi,[30,v] J. Reich,[56] F. Reiss,[20] Z. Ren,[7] P. K. Resmi,[65] M. Ribalda Galvez,[46] R. Ribatti,[51] G. Ricart,[15,12] D. Riccardi,[35,j] S. Ricciardi,[59] K. Richardson,[66] M. Richardson-Slipper,[57] F. Riehn,[19] K. Rinnert,[62] P. Robbe,[14,50] G. Robertson,[61] E. Rodrigues,[62] A. Rodriguez Alvarez,[46] E. Rodriguez Fernandez,[48] J. A. Rodriguez Lopez,[78] E. Rodriguez Rodriguez,[50] J. Roensch,[19] A. Rogachev,[44] A. Rogovskiy,[59] D. L. Rolf,[19] P. Roloff,[50] V. Romanovskiy,[67] A. Romero Vidal,[48] G. Romolini,[26,50] F. Ronchetti,[51] T. Rong,[6] M. Rotondo,[28] S. R. Roy,[22] M. S. Rudolph,[70] M. Ruiz Diaz,[22] R. A. Ruiz Fernandez,[48] J. Ruiz Vidal,[84] J. J. Saavedra-Arias,[9] J. J. Saborido Silva,[48] S. E. R. Sacha Emile R.,[50] N. Sagidova,[44] D. Sahoo,[81] N. Sahoo,[55] B. Saitta,[32] M. Salomoni,[31,50,b] I. Sanderswood,[49] R. Santacesaria,[36] C. Santamarina Rios,[48] M. Santimaria,[28] L. Santoro,[2] E. Santovetti,[37] A. Saputi,[26,50] D. Saranin,[44] A. Sarnatskiy,[83] G. Sarpis,[50] M. Sarpis,[82] C. Satriano,[36] A. Satta,[37] M. Saur,[75] D. Savrina,[44] H. Sazak,[17] F. Sborzacchi,[50,28] A. Scarabotto,[19] S. Schael,[17] S. Scherl,[62] M. Schiller,[22] H. Schindler,[50] M. Schmelling,[21] B. Schmidt,[50] N. Schmidt,[69] S. Schmitt,[66] H. Schmitz,[18] O. Schneider,[51] A. Schopper,[63] N. Schulte,[19] M. H. Schune,[14] G. Schwering,[17] B. Sciascia,[28] A. Sciuccati,[50] G. Scriven,[84] I. Segal,[80] S. Sellam,[48] A. Semennikov,[44] T. Senger,[52] M. Senghi Soares,[39] A. Sergi,[29,i] N. Serra,[52] L. Sestini,[27] A. Seuthe,[19] B. Sevilla Sanjuan,[47] Y. Shang,[6] D. M. Shangase,[88] M. Shapkin,[44] R. S. Sharma,[70] I. Shchemerov,[44] L. Shchutska,[51] T. Shears,[62] L. Shekhtman,[44] Z. Shen,[38] S. Sheng,[5,7] V. Shevchenko,[44] B. Shi,[7] Q. Shi,[7] W. S. Shi,[74] Y. Shimizu,[14] E. Shmanin,[25] R. Shorkin,[44] J. D. Shupperd,[70] R. Silva Coutinho,[2] G. Simi,[33,u] S. Simone,[24,p] M. Singha,[81] N. Skidmore,[58] T. Skwarnicki,[70] M. W. Slater,[55] E. Smith,[66] K. Smith,[69] M. Smith,[63] L. Soares Lavra,[60] M. D. Sokoloff,[67] F. J. P. Soler,[61] A. Solomin,[56] A. Solovev,[44] K. Solovieva,[20] N. S. Sommerfeld,[18] R. Song,[1] Y. Song,[51] Y. Song,[4,l] Y. S. Song,[6] F. L. Souza De Almeida,[46] B. Souza De Paula,[3] K. M. Sowa,[40] E. Spadaro Norella,[29,i] E. Spedicato,[25] J. G. Speer,[19] P. Spradlin,[61] F. Stagni,[50] M. Stahl,[80] S. Stahl,[50] S. Stanislaus,[65] M. Stefaniak,[89] E. N. Stein,[50] O. Steinkamp,[52] D. Strekalina,[44] Y. Su,[7] F. Suljik,[65] J. Sun,[32] J. Sun,[64] L. Sun,[76] D. Sundfeld,[2] W. Sutcliffe,[52] P. Svihra,[79] V. Svintozelskyi,[49] K. Swientek,[40] F. Swystun,[57] A. Szabelski,[42] T. Szumlak,[40] Y. Tan,[4] Y. Tang,[76] Y. T. Tang,[7] M. D. Tat,[22] J. A. Teijeiro Jimenez,[48] A. Terentev,[44] F. Terzuoli,[35,x] F. Teubert,[50] E. Thomas,[50] D. J. D. Thompson,[55] A. R. Thomson-Strong,[60] H. Tilquin,[63] V. Tisserand,[11] S. T'Jampens,[10] M. Tobin,[5,50] T. T. Todorov,[20] L. Tomassetti,[26,f] G. Tonani,[30] X. Tong,[6] T. Tork,[30] D. Torres Machado,[2] L. Toscano,[19] D. Y. Tou,[4,l] C. Trippl,[47] G. Tuci,[22] N. Tuning,[38] L. H. Uecker,[22] A. Ukleja,[40] D. J. Unverzagt,[22] A. Upadhyay,[50] B. Urbach,[60] A. Usachov,[38] A. Ustyuzhanin,[44] U. Uwer,[22] V. Vagnoni,[25,50] A. Vaitkevicius,[82] V. Valcarce Cadenas,[48] G. Valenti,[25] N. Valls Canudas,[50] J. van Eldik,[50] H. Van Hecke,[69] E. van Herwijnen,[63] C. B. Van Hulse,[48,y] R. Van Laak,[51] M. van Veghel,[84] G. Vasquez,[52] R. Vazquez Gomez,[46] P. Vazquez Regueiro,[48] C. Vázquez Sierra,[45] S. Vecchi,[26] J. Velilla Serna,[49] J. J. Velthuis,[56] M. Veltri,[27,z] A. Venkateswaran,[51] M. Verdoglia,[32] M. Vesterinen,[58] W. Vetens,[70] D. Vico Benet,[65] P. Vidrier Villalba,[46] M. Vieites Diaz,[48] X. Vilasis-Cardona,[47] E. Vilella Figueras,[62] A. Villa,[25] P. Vincent,[16] B. Vivacqua,[3] F. C. Volle,[55] D. vom Bruch,[13] N. Voropaev,[44] K. Vos,[84] C. Vrahas,[60] J. Wagner,[19] J. Walsh,[35] E. J. Walton,[1,58] G. Wan,[6] A. Wang,[7] B. Wang,[5] C. Wang,[22] G. Wang,[8] H. Wang,[75] J. Wang,[7] J. Wang,[5] J. Wang,[4,l] J. Wang,[76] M. Wang,[50] N. W. Wang,[7] R. Wang,[56] X. Wang,[8] X. Wang,[74] X. W. Wang,[63] Y. Wang,[77] Y. Wang,[6] Y. H. Wang,[75] Z. Wang,[14] Z. Wang,[30] J. A. Ward,[58,1] M. Waterlaat,[50] N. K. Watson,[55] D. Websdale,[63] Y. Wei,[6] Z. Weida,[7] J. Wendel,[45] B. D. C. Westhenry,[56] C. White,[57] M. Whitehead,[61] E. Whiter,[55] A. R. Wiederhold,[64] D. Wiedner,[19] M. A. Wiegertjes,[38] C. Wild,[65] G. Wilkinson,[65,50] M. K. Wilkinson,[67] M. Williams,[66] M. J. Williams,[50] M. R. J. Williams,[60] R. Williams,[57] S. Williams,[56] Z. Williams,[56] F. F. Wilson,[59] M. Winn,[12] W. Wislicki,[42] M. Witek,[41] L. Witola,[19] T. Wolf,[22] E. Wood,[57]

G. Wormser,[14] S. A. Wotton,[57] H. Wu,[70] J. Wu,[8] X. Wu,[76] Y. Wu,[6,57] Z. Wu,[7] K. Wyllie,[50] S. Xian,[74] Z. Xiang,[5] Y. Xie,[8] T. X. Xing,[30] A. Xu,[35,j] L. Xu,[4,l] M. Xu,[50] Z. Xu,[50] Z. Xu,[7] Z. Xu,[5] S. Yadav,[26] K. Yang,[63] X. Yang,[6] Y. Yang,[7] Y. Yang,[81] Z. Yang,[6] V. Yeroshenko,[14] H. Yeung,[64] H. Yin,[8] X. Yin,[7] C. Y. Yu,[6] J. Yu,[73] X. Yuan,[5] Y Yuan,[5,7] J. A. Zamora Saa,[72] M. Zavertyaev,[21] M. Zdybal,[41] F. Zenesini,[25] C. Zeng,[5,7] M. Zeng,[4,l] C. Zhang,[6] D. Zhang,[8] J. Zhang,[7] L. Zhang,[4,l] R. Zhang,[8] S. Zhang,[65] S. L. Zhang,[73] Y. Zhang,[6] Y. Z. Zhang,[4,l] Z. Zhang,[4,l] Y. Zhao,[22] A. Zhelezov,[22] S. Z. Zheng,[6] X. Z. Zheng,[4,l] Y. Zheng,[7] T. Zhou,[6] X. Zhou,[8] Y. Zhou,[7] V. Zhovkovska,[58] L. Z. Zhu,[7] X. Zhu,[4,l] X. Zhu,[8] Y. Zhu,[17] V. Zhukov,[17] J. Zhuo,[49] Q. Zou,[5,7] D. Zuliani,[33,u] and G. Zunica[28]

(LHCb Collaboration)

[1]*School of Physics and Astronomy, Monash University, Melbourne, Australia*
[2]*Centro Brasileiro de Pesquisas Físicas (CBPF), Rio de Janeiro, Brazil*
[3]*Universidade Federal do Rio de Janeiro (UFRJ), Rio de Janeiro, Brazil*
[4]*Department of Engineering Physics, Tsinghua University, Beijing, China*
[5]*Institute Of High Energy Physics (IHEP), Beijing, China*
[6]*School of Physics State Key Laboratory of Nuclear Physics and Technology, Peking University, Beijing, China*
[7]*University of Chinese Academy of Sciences, Beijing, China*
[8]*Institute of Particle Physics, Central China Normal University, Wuhan, Hubei, China*
[9]*Consejo Nacional de Rectores (CONARE), San Jose, Costa Rica*
[10]*Université Savoie Mont Blanc, CNRS, IN2P3-LAPP, Annecy, France*
[11]*Université Clermont Auvergne, CNRS/IN2P3, LPC, Clermont-Ferrand, France*
[12]*Université Paris-Saclay, Centre d'Etudes de Saclay (CEA), IRFU, Saclay, France, Gif-Sur-Yvette, France*
[13]*Aix Marseille University, CNRS/IN2P3, CPPM, Marseille, France*
[14]*Université Paris-Saclay, CNRS/IN2P3, IJCLab, Orsay, France*
[15]*Laboratoire Leprince-Ringuet, CNRS/IN2P3, Ecole Polytechnique, Institut Polytechnique de Paris, Palaiseau, France*
[16]*Laboratoire de Physique Nucléaire et de Hautes Énergies (LPNHE), Sorbonne Université, CNRS/IN2P3, F-75005 Paris, France*
[17]*I. Physikalisches Institut, RWTH Aachen University, Aachen, Germany*
[18]*Universität Bonn—Helmholtz-Institut für Strahlen und Kernphysik, Bonn, Germany*
[19]*Fakultät Physik, Technische Universität Dortmund, Dortmund, Germany*
[20]*Physikalisches Institut, Albert-Ludwigs-Universität Freiburg, Freiburg, Germany*
[21]*Max-Planck-Institut für Kernphysik (MPIK), Heidelberg, Germany*
[22]*Physikalisches Institut, Ruprecht-Karls-Universität Heidelberg, Heidelberg, Germany*
[23]*School of Physics, University College Dublin, Dublin, Ireland*
[24]*INFN Sezione di Bari, Bari, Italy*
[25]*INFN Sezione di Bologna, Bologna, Italy*
[26]*INFN Sezione di Ferrara, Ferrara, Italy*
[27]*INFN Sezione di Firenze, Firenze, Italy*
[28]*INFN Laboratori Nazionali di Frascati, Frascati, Italy*
[29]*INFN Sezione di Genova, Genova, Italy*
[30]*INFN Sezione di Milano, Milano, Italy*
[31]*INFN Sezione di Milano-Bicocca, Milano, Italy*
[32]*INFN Sezione di Cagliari, Monserrato, Italy*
[33]*INFN Sezione di Padova, Padova, Italy*
[34]*INFN Sezione di Perugia, Perugia, Italy*
[35]*INFN Sezione di Pisa, Pisa, Italy*
[36]*INFN Sezione di Roma La Sapienza, Roma, Italy*
[37]*INFN Sezione di Roma Tor Vergata, Roma, Italy*
[38]*Nikhef National Institute for Subatomic Physics, Amsterdam, Netherlands*
[39]*Nikhef National Institute for Subatomic Physics and VU University Amsterdam, Amsterdam, Netherlands*
[40]*AGH–University of Krakow, Faculty of Physics and Applied Computer Science, Kraków, Poland*
[41]*Henryk Niewodniczanski Institute of Nuclear Physics Polish Academy of Sciences, Kraków, Poland*
[42]*National Center for Nuclear Research (NCBJ), Warsaw, Poland*
[43]*Horia Hulubei National Institute of Physics and Nuclear Engineering, Bucharest-Magurele, Romania*
[44]*Authors affiliated with an institute formerly covered by a cooperation agreement with CERN*
[45]*Universidade da Coruña, A Coruña, Spain*
[46]*ICCUB, Universitat de Barcelona, Barcelona, Spain*

[47]La Salle, Universitat Ramon Llull, Barcelona, Spain
[48]Instituto Galego de Física de Altas Enerxías (IGFAE), Universidade de Santiago de Compostela, Santiago de Compostela, Spain
[49]Instituto de Fisica Corpuscular, Centro Mixto Universidad de Valencia—CSIC, Valencia, Spain
[50]European Organization for Nuclear Research (CERN), Geneva, Switzerland
[51]Institute of Physics, Ecole Polytechnique Fédérale de Lausanne (EPFL), Lausanne, Switzerland
[52]Physik-Institut, Universität Zürich, Zürich, Switzerland
[53]NSC Kharkiv Institute of Physics and Technology (NSC KIPT), Kharkiv, Ukraine
[54]Institute for Nuclear Research of the National Academy of Sciences (KINR), Kyiv, Ukraine
[55]School of Physics and Astronomy, University of Birmingham, Birmingham, United Kingdom
[56]H.H. Wills Physics Laboratory, University of Bristol, Bristol, United Kingdom
[57]Cavendish Laboratory, University of Cambridge, Cambridge, United Kingdom
[58]Department of Physics, University of Warwick, Coventry, United Kingdom
[59]STFC Rutherford Appleton Laboratory, Didcot, United Kingdom
[60]School of Physics and Astronomy, University of Edinburgh, Edinburgh, United Kingdom
[61]School of Physics and Astronomy, University of Glasgow, Glasgow, United Kingdom
[62]Oliver Lodge Laboratory, University of Liverpool, Liverpool, United Kingdom
[63]Imperial College London, London, United Kingdom
[64]Department of Physics and Astronomy, University of Manchester, Manchester, United Kingdom
[65]Department of Physics, University of Oxford, Oxford, United Kingdom
[66]Massachusetts Institute of Technology, Cambridge, Massachusetts, USA
[67]University of Cincinnati, Cincinnati, Ohio, USA
[68]University of Maryland, College Park, Maryland, USA
[69]Los Alamos National Laboratory (LANL), Los Alamos, New Mexico, USA
[70]Syracuse University, Syracuse, New York, USA
[71]Pontifícia Universidade Católica do Rio de Janeiro (PUC-Rio),
Rio de Janeiro, Brazil (associated with Universidade Federal do Rio de Janeiro (UFRJ), Rio de Janeiro, Brazil)
[72]Universidad Andres Bello, Santiago, Chile (associated with Physik-Institut, Universität Zürich, Zürich, Switzerland)
[73]School of Physics and Electronics, Hunan University,
Changsha City, China (associated with Institute of Particle Physics, Central China Normal University, Wuhan, Hubei, China)
[74]State Key Laboratory of Nuclear Physics and Technology, South China Normal University,
Guangzhou, China (associated with Department of Engineering Physics, Tsinghua University, Beijing, China)
[75]Lanzhou University, Lanzhou, China (associated with Institute of High Energy Physics (IHEP), Beijing, China)
[76]School of Physics and Technology, Wuhan University,
Wuhan, China (associated with Department of Engineering Physics, Tsinghua University, Beijing, China)
[77]Henan Normal University,
Xinxiang, China (associated with Institute of Particle Physics, Central China Normal University, Wuhan, Hubei, China)
[78]Departamento de Fisica, Universidad Nacional de Colombia,
Bogota, Colombia (associated with Laboratoire de Physique Nucléaire et de Hautes Énergies (LPNHE), Sorbonne Université, CNRS/IN2P3, F-75005 Paris, France)
[79]Institute of Physics of the Czech Academy of Sciences,
Prague, Czech Republic (associated with Department of Physics and Astronomy, University of Manchester, Manchester, United Kingdom)
[80]Ruhr Universitaet Bochum,
Fakultaet für Physik und Astronomie, Bochum, Germany (associated with Fakultät Physik, Technische Universität Dortmund, Dortmund, Germany)
[81]Eotvos Lorand University, Budapest, Hungary (associated with European Organization for Nuclear Research (CERN), Geneva, Switzerland)
[82]Faculty of Physics, Vilnius University,
Vilnius, Lithuania (associated with Physikalisches Institut, Albert-Ludwigs-Universität Freiburg, Freiburg, Germany)
[83]Van Swinderen Institute, University of Groningen,
Groningen, Netherlands (associated with Nikhef National Institute for Subatomic Physics, Amsterdam, Netherlands)
[84]Universiteit Maastricht, Maastricht, Netherlands (associated with Nikhef National Institute for Subatomic Physics, Amsterdam, Netherlands)
[85]Tadeusz Kosciuszko Cracow University of Technology,
Cracow, Poland (associated with Henryk Niewodniczanski Institute of Nuclear Physics Polish Academy of Sciences, Kraków, Poland)
[86]Department of Physics and Astronomy, Uppsala University, Uppsala, Sweden (associated with School of Physics and Astronomy, University of Glasgow, Glasgow, United Kingdom)

[87]*Taras Schevchenko University of Kyiv, Faculty of Physics, Kyiv, Ukraine (associated with Université Paris-Saclay, CNRS/IN2P3, IJCLab, Orsay, France)*
[88]*University of Michigan, Ann Arbor, Michigan, USA (associated with Syracuse University, Syracuse, New York, USA)*
[89]*Ohio State University, Columbus, Ohio, USA (associated with Los Alamos National Laboratory (LANL), Los Alamos, New Mexico, USA)*

[a]Also at Lamarr Institute for Machine Learning and Artificial Intelligence, Dortmund, Germany.
[b]Also at Università degli Studi di Milano-Bicocca, Milano, Italy.
[c]Also at Università di Roma Tor Vergata, Roma, Italy.
[d]Also at Università di Modena e Reggio Emilia, Modena, Italy.
[e]Also at Department of Physics and Astronomy, University of Victoria, Victoria, British Columbia, Canada.
[f]Also at Università di Ferrara, Ferrara, Italy.
[g]Also at Universidade Estadual de Campinas (UNICAMP), Campinas, Brazil.
[h]Also at Università di Bologna, Bologna, Italy.
[i]Also at Università di Genova, Genova, Italy.
[j]Also at Scuola Normale Superiore, Pisa, Italy.
[k]Also at Università degli Studi di Milano, Milano, Italy.
[l]Also at Center for High Energy Physics, Tsinghua University, Beijing, China.
[m]Also at Universidad Nacional Autónoma de Honduras, Tegucigalpa, Honduras.
[n]Also at Università di Cagliari, Cagliari, Italy.
[o]Also at Centro Federal de Educacão Tecnológica Celso Suckow da Fonseca, Rio De Janeiro, Brazil.
[p]Also at Università di Bari, Bari, Italy.
[q]Also at Università di Perugia, Perugia, Italy.
[r]Also at LIP6, Sorbonne Université, Paris, France.
[s]Also at Università di Pisa, Pisa, Italy.
[t]Also at Hangzhou Institute for Advanced Study, UCAS, Hangzhou, China.
[u]Also at Università di Padova, Padova, Italy.
[v]Also at Università di Bergamo, Bergamo, Italy.
[w]Also at Universidad de Ingeniería y Tecnología (UTEC), Lima, Peru.
[x]Also at Università di Siena, Siena, Italy.
[y]Also at Universidad de Alcalá, Alcalá de Henares, Spain.
[z]Also at Università di Urbino, Urbino, Italy.